ORIGINAL PAPER

A.K.A. Pryde · M.T. Dove

On the Sequence of Phase Transitions in Tridymite

Abstract We consider the phase transitions in tridymite from the perspective of the rigid unit mode model. The rigid unit modes are the low-frequency phonons of a crystal structure that consists of an infinite framework of tetrahedra linked at corners, that can propagate without the tetrahedra distorting. Because they give distortions of the structure with a low energy cost they are the natural soft modes for displacive phase transitions. We consider the normal phase transition sequence in tridymite on cooling, HP LHP ..., as a successive condensation of rigid unit modes acting as soft modes. Some of the low-temperature phases (e.g. MX-1) arise as rigid unit mode distortions of the high-temperature structure and do not follow the sequence of phases found at higher temperatures. We are able to account for all the commensurate phases and some of the modulated phase within the framework of the rigid unit mode model.

Key words Tridymite · Rigid unit modes · Phase transitions

Introduction

The silica polymorph tridymite is notable for the surprisingly high number of phases which have been reported to exist. Recent work by Cellai et al. (1995) has helped to clarify the long sequence of phase transitions by which they are related, by collating results from the many experimental studies on tridymite over the years (Cellai et al. 1994; de Dombal and Carpenter 1993; Dollase 1967; Dollase and Baur 1976; Kihara 1977, 1978; Löns and Hoffmann 1987; Nukui et al. 1978). This sequence, illustrated in Fig. 1, comprises a total of seven different phases. The crystallographic data and crystal structures for these phases are reproduced in Table 1 and Fig. 2 respectively.

A.K.A. Pryde · M.T. Dove (✉)
Department of Earth Sciences, University of Cambridge,
Downing Street, Cambridge, UK, CB2 3EQ
Fax: +44 1223 333450, e-mail: martin@esc.cam.ac.uk

The highest-temperature phase of tridymite is the ideal HP phase (space group $P6_3\,mmc$), which transforms on cooling to another hexagonal phase, LHP tridymite (space group $P6_322$). The preservation of the hexagonal lattice and the small continuous changes in the lattice parameters had led to the failure of many workers to notice the LHP phase. The transition was first detected by Cellai et al. (1994) from careful measurements of the associated specific heat anomaly using differential scanning calorimetry (DSC). The LHP phase undergoes a transition to a C-centred orthorhombic structure, OC tridymite (space group $C222_1$), which then transforms to a metrically orthorhombic phase with an incommensurate modulation, OS tridymite. The structure of the OS phase has not been measured, but the wave vector characterising the modulation is known to have the form $\mathbf{k}=\mu a^*$ where μ is a function of temperature (Nukui et al. 1978). Therefore the OS phase comprises a series of structures which are $n \times 1 \times 1$ supercells of the OC phase, where $n=1/\mu$ and is not necessarily an integer. On further cooling there is a transition to the OP phase (space group $P2_12_12_1$), which is a $3 \times 1 \times 1$ supercell of the OC phase, with a primitive orthorhombic
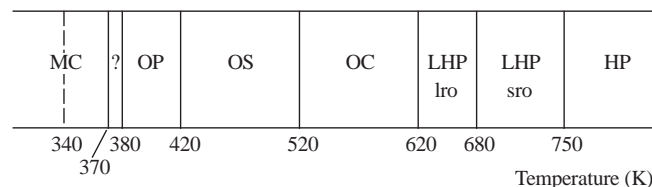

Fig. 1 The sequence of phase transitions in annealed tridymite from the Steinbach meteorite, as reported by Cellai et al. (1995). The *dashed line* in the MC stability field indicates the transition to the MC phase from the MX-1 phase. The abbreviations *lro* and *sro* in the LHP phase refer to long- and short-range order. This study suggests that the LHP phase truly exists in the *lro* temperature range, and the *sro* range corresponds to the temperatures over which the RUM responsible for the HP–LHP transition softens. The HP–LHP transition then occurs at 680 K, coinciding with the C_P anomaly characteristic of a second order phase transition: *HP*, hexagonal primitive; *OS*, orthorhombic superstructure; *LHP*, low hexagonal primitive; *OP*, orthorhombic primitive; *OC*, orthorhombic C-centred; *MC*, monoclinic C-centred

Table 1 Some crystallographic data for the phases of tridymite, Fig. 2

Phase	Space group	Lattice parameters (Å)	T (K)	Reference and tridymite source
HP	$P6_3/mmc$	a=5.05 c=8.27	733	Kihara (1978) Fired silica brick
LHP	$P6_322$	a=5.05 c=8.26	673	Celai et al. (1994) Steinbach meteorite
OC	$C222_1$	a=8.74 b=5.04 c=8.24	493	Dollase (1967) Steinbach meteorite
OS	Incommensurately modulated, metrically orthorhombic structure	a=95–65[a] b=5.02 c=8.18	423–463	Nukui et al. (1978) Synthetic
		a=105–65[a]	380–453	Dollase (1967) Steinbach meteorite
OP	$P2_12_12_1$	a=26.171 b=4.99 c=8.20	428	Kihara (1977) Fired silica brick
MC[b]	Cc	a=18.52 b=5.00 c=23.81 β=105.82°	295	Dollase and Baur (1976) Steinbach meteorite
MX-1	Cc (Average structure)	a=8.60 b=5.01 c=16.43 β=91.51°	295	Löns and Hoffmann (1987), Graetsch and Topalovic-Dierdorf (1996) Synthetic
MX-1	$C1$ (Modulated structure)	a=8.60 b=15.02 c=16.43 β=91.51°	295	Löns and Hoffmann (1987), Graetsch and Topalovic-Dierdorf (1996) Synthetic

[a] The range of lattice parameters is due to existence of a series of OS phases associated with different modulating wave vectors along **a***
[b] Hoffmann (1967) and Kato and Nukui (1976) setting is a=18.49 Å; b=4.99 Å; c=25.83 Å; β=117.8°

lattice. However, the OP phase is only observed in tridymite samples which have been annealed in the stability field of the HP phase. In other samples the transition sequence proceeds directly from the OS phase to the next phase in the sequence, the monoclinic C-centred phase MC tridymite (space group Cc). There is also a C-centred triclinic phase of tridymite, MX-1 tridymite (space group $C1$). This can be described as an average structure combined with a modulation which results in a tripling of the b lattice parameter belonging to the average structure. This phase is only obtained by quenching a tridymite sample from temperatures above 400 K to around 250 K, or by grinding the MC phase. On heating, MX-1 tridymite transforms to the MC phase, as indicated by the dashed line in the stability field of MC tridymite in Fig. 1.

The basic crystal structure of tridymite is closely related to that of the other high-temperature silica polymorph, cristobalite. Both structures are based on the same structural unit-layers which comprise six-fold rings of corner-sharing SiO_4 tetrahedra. The difference arises from the manner in which these layers are stacked together. But despite this fundamental similarity, the phase transition behaviour of cristobalite is very different from tridymite. On cooling the high-temperature ideal phase, β-cristobalite, there is only one phase transition, and this is accompanied by a substantial volume reduction of around 5% (Schmahl et al. 1992). By contrast, the phase transitions experienced by tridymite are accompa-

Table 2 The relative volumes of the tridymite phases with respect to the HP phase, expressed as a percentage. For comparison, the volume of α-cristobalite is less than 95% of the volume of β-cristobalite, showing that the volume changes associated with the phase transitions in tridymite are relatively small

| Phase	Cell volume relative to HP phase, %
HP	100.00
LHP	99.80
OC	99.28
OP	97.51
MC[a]	96.79
MC[b]	96.20
MX-1	96.75

[a] Dollase and Baur (1976)
[b] Kato and Nukui (1976)

nied by much smaller volume changes (Table 2). Even at the end of the phase transition sequence, in the lowest symmetry phases, MC and MX-1 tridymite, the cell volumes are still greater than 96% of the HP tridymite cell volume. By making this comparison it becomes apparent that the structural changes accompanying the many phase transitions in tridymite are relatively slight, and the accompanying energy differences will be relatively small also.

This may explain why the behaviour of tridymite is notoriously sensitive to the structural defects which may be

Fig. 2 The crystal structures of equivalent layers in six commensurate tridymite phases and also the average structure of the MX-1 phase. The SiO$_4$ tetrahedra are shown as *shaded polyhedra* and the projections of the unit cells are *outlined*. For *HP*, *LHP*, *OC*, *OP* and *MX-1* tridymite the view is down [001] but for the *MC* structure the equivalent is view is down [101]. Crystallographic data and references pertaining to these structures are presented in Table 1 and the relative volumes of the structures are compared in Table 2
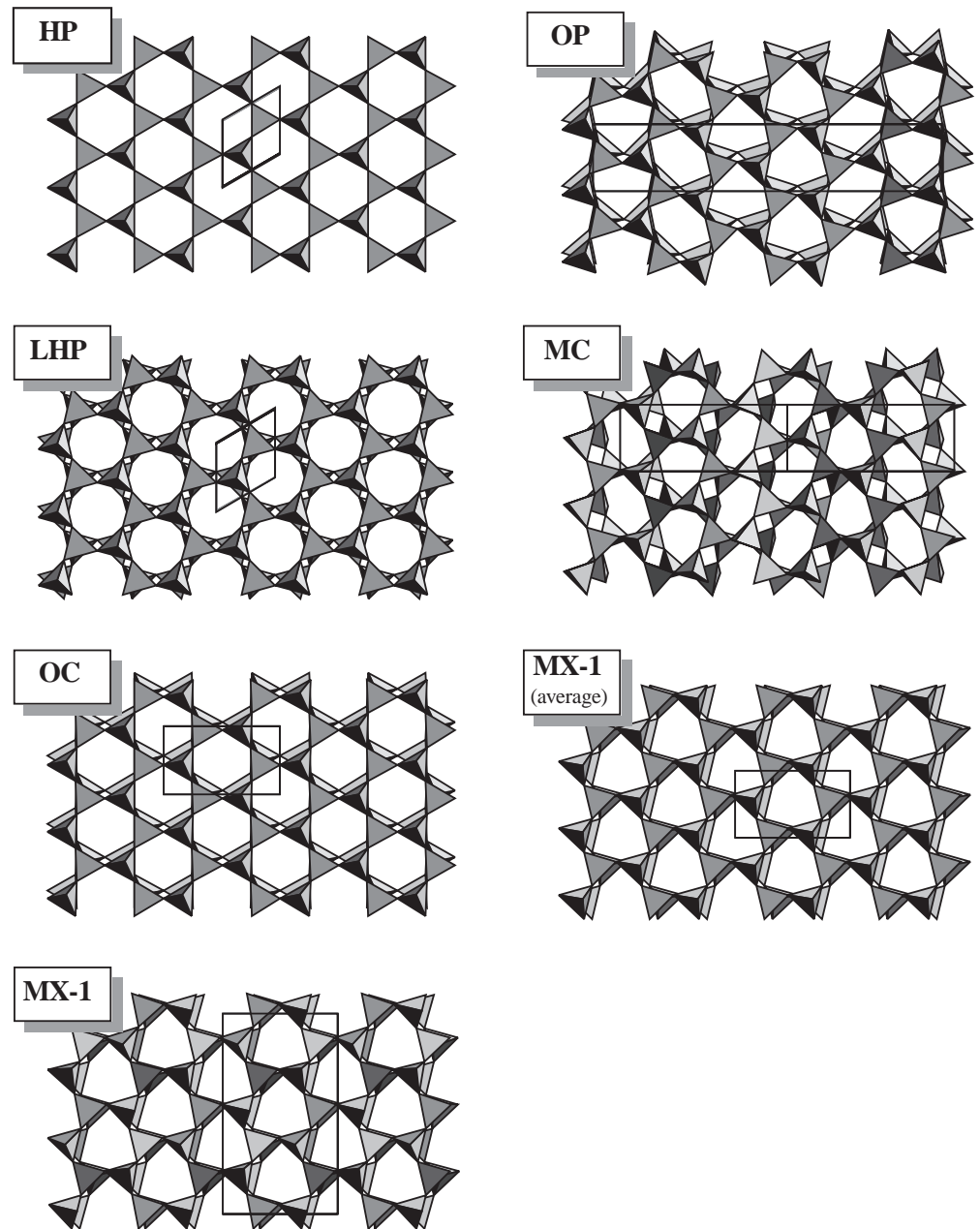
present in different samples, i.e. faults in the stacking sequence and the presence of impurities as interstitial cations in the framework. For example, the requirement to anneal a tridymite sample in order to observe the OP phase, suggests that the presence of stacking faults, even in small concentrations, causes sufficient perturbation of the energy of the system that the OP structure can not compete successfully against the OS and MC phases to become the stable phase at any temperature. Grinding can also introduce stacking faults, and Graetsch and Flörke (1991) found that in tridymite samples which had been ground, the temperature range over which the OP phase was observed was reduced in favour of a wider temperature range for the OS phase.

The aim of this study is to develop a theoretical framework to describe the phase transitions in tridymite in terms of the rigid unit mode model (Giddy et al. 1993; Dove et al. 1995; Hammonds et al. 1996; Dove 1997a). This is achieved by determining the rigid unit modes (RUMs) that act as soft modes for the displacive phase transitions. Information about these RUMs, such as their symmetry and the structural changes they cause, can be linked to measurable quantities such as specific heat anomalies and diffuse scattering. As a result, experimental measurements can be used to support the picture which emerges, and in return this theoretical framework can be used to ensure that experimental observations are attributed to the correct effect in tridymite.

We consider data gathered by four experimental studies on tridymite over wide temperature ranges (Cellai et al. 1994; de Dombal and Carpenter 1993; Graetsch and Flörke 1991; Kihara 1978). Kihara (1978) reports results from X-ray diffraction studies of single crystals of tridymite obtained from refractory silica bricks which had been fired for a long time in the temperature range 1030–1740 K, in which the stable polymorph of silica is HP tridymite. Graetsch and Flörke (1991) synthesized crystals of MC tridymite from high-purity silica glass and then used quenching and grinding (independently) to obtain the MX-1 phase. Synthetic tridymite samples tend to be more inclined to stacking faults than tridymite from refractory bricks, due to their shorter annealing time. Graetsch and Flörke (1991) present the results of X-ray powder diffraction using both the MC and MX-1 phases as the starting phase, then heating. The studies reported in both de Dombal and Carpenter (1993) and Cellai et al. (1994) used tridymite samples originating from the Steinbach meteorite. This was discovered in Germany in 1724, and is found to be a fairly pure source of tridymite, containing impurities amounting to around 0.5% (Cellai et al. 1994). Both studies used X-ray diffraction and differential scanning calorimetry (DSC) to investigate the transitions in tridymite, but Cellai et al. (1994) used single crystals, whereas de Dombal and Carpenter (1993) used powdered samples. In both cases, experiments were performed on an unannealed sample, but Cellai et al. (1994) repeated them on a sample which had been annealed in the stability field of the HP phase.

The rigid unit mode model

At the heart of the rigid unit mode model is the possibility for some of the phonon modes in a crystal structure that is made from a framework of linked polyhedra (e.g. SiO_4 tetrahedra) to propagate without the polyhedra distorting. Since any distortion of the polyhedra will cost energy, phonon modes that do not require these distortions will have low frequency. A displacive phase transition will involve a freezing-in of a low-frequency phonon (the 'soft mode', Dove 1997b), and so the low-frequency RUMs are natural candidates for soft modes that will drive displacing phase transitions in silicates (Giddy et al. 1993). This point has been documented in some detail for quartz, cristobalite and other examples by Hammonds et al. (1996).

In this study we will determine the RUMs for different phases of tridymite. This is accomplished using our 'split-atom' method (Giddy et al. 1993) which has been conveniently programmed using molecular lattice dynamics formalism (Hammonds et al. 1994). This approach gives the number of RUMs for any chosen wave vector, together with the eigenvectors of the RUMs which contain information about the symmetry.

The soft-mode model for a phase transition represents the change in symmetry as arising from a condensation of a normal mode of the high-symmetry phase, so that the structure of the low-symmetry phase can be described as arising from the modulation of the structure of the high-symmetry phase by the eigenvector of the soft mode. In some cases the classical soft-mode picture is a simplification of the real situation, since the soft mode in the high-symmetry can be overdamped, giving rise to considerable structural disorder. This is the case in some perovskites (see Dove 1997b for a discussion on this point), and the analysis of the phase transition in cristobalite from a number of theoretical (Swainson and Dove 1995; Hammonds et al. 1996) and experimental (Swainson and Dove 1993; Dove et al. 1997) perspectives shows this to be the case also for β-cristobalite. Indeed, evidence from experiment (Keen and Dove submitted 1998) and simulation (Pryde and Dove 1998) studies shows this to be the case also for the high-temperature phases of tridymite. Nevertheless, the distortions that accompany these phase transitions can still be adequately described in terms of a condensing soft mode, and it is within this spirit that we exploit the concepts of the soft-mode model here.

The HP-LHP transition

The HP phase of tridymite has a large number of RUMs whose wave vectors are located at special points, along special lines and on special planes in reciprocal space, Table 3. Each of these RUMs has the potential to act as a soft mode for a phase transition to another crystal structure, in practice only one RUM will act as a soft mode for the phase transition to the LHP phase, but we will show that some of the other RUMs are required for some of the other phase transitions found in tridymite. The HP-LHP transition does not appreciably alter the size of the unit cell, which remains hexagonal and continues to contain four SiO_4 tetrahedra, so the soft mode will have wave vector **k**=0, which is conventionally labelled as the Γ-point in the Brillouin zone.

An analysis of the eigenvectors of the RUMs at Γ for HP tridymite shows that the six RUMs comprise two non-degenerate modes, which are labelled according to their symmetry as Γ_1^- (A_{1u}) and Γ_3^- (B_{1u}), and two doubly-degenerate modes, Γ_5^- (E_{1u}) and Γ_6^- (E_{2u}). In this notation, a superscript minus (or plus) sign indicates that the mode destroys (or preserves) the centre of symmetry present

Table 3 Rigid unit modes in HP tridymite: A, non-degenerate; E, doubly-degenerate; T, triply-degenerate; F quadruply-degenerate (from Hammonds et al. 1996)

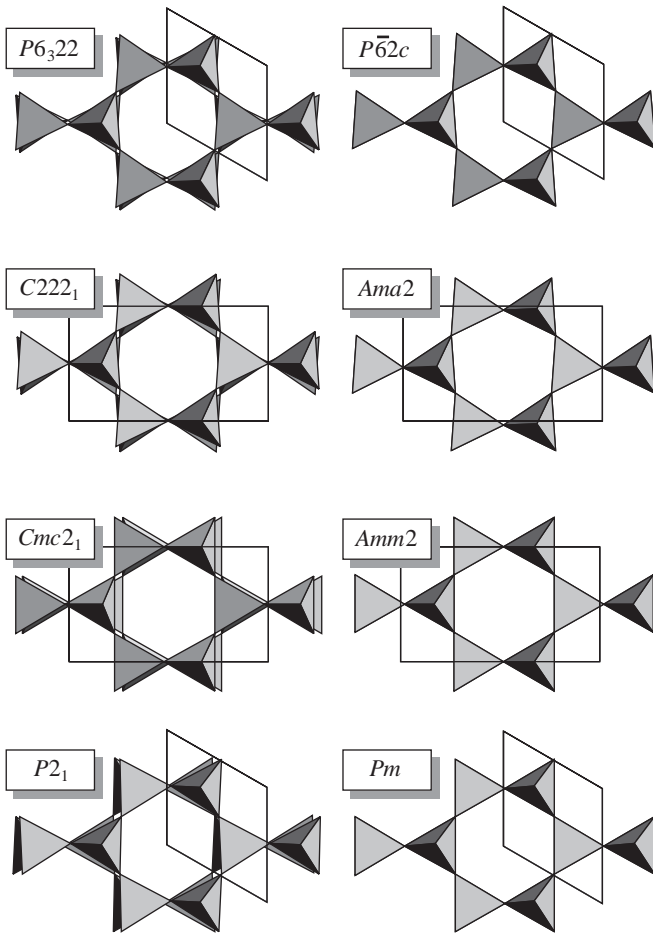| Special points		Special lines		Special planes	
Γ $(0, 0, 0)$	$2A+2E$	Σ $(\xi, 0, 0)$	$3A$	$(\xi, \zeta, 0)$	A
M $(\frac{1}{2}, 0, 0)$	$3A$	Λ $(\xi, \xi, 0)$	A	$(\xi, 0, \zeta)$	$2A$
K $(\frac{1}{3}, \frac{1}{3}, 0)$	A	Δ $(0, 0, \xi)$	$2A+2E$		
A $(0, 0, \frac{1}{2})$	$E+F$	R $(\xi, 0, \frac{1}{2})$	E		
L $(\frac{1}{2}, 0, \frac{1}{2})$	E	T $(\frac{1}{2}-\xi, 2\xi, 0)$	A		
H $(\frac{1}{3}, \frac{1}{3}, \frac{1}{2})$	$2A$	U $(\frac{1}{2}, 0, \xi)$	$2A$		

Fig. 3 Crystal structures with the eight space group symmetries which can be derived from the HP structure, space group $P6_3mmc$, via the six RUMs at the Γ-point. These are the singlets Γ_1^- ($P6_322$); and Γ_3^- ($p\bar{6}2c$); and the doublets Γ_5^- ($C222_1$, $Cmc2_1$, $P2_1$); and Γ_6^- ($Amm2$, $Ama2$, Pm)
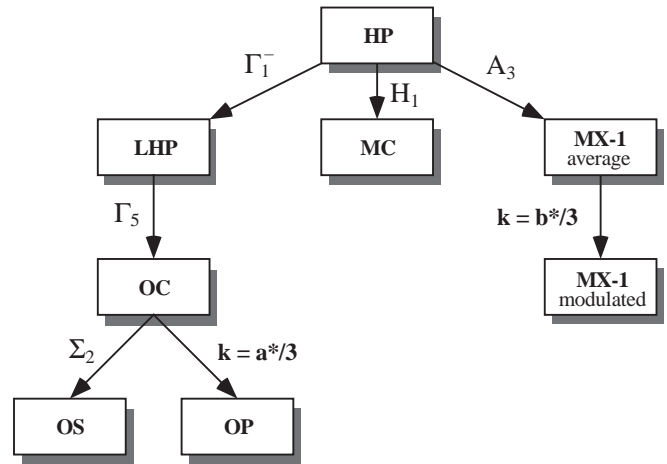

Fig. 4 Schematic diagram showing the lineage of the phases of tridymite in terms of parent phases and the wave vector and symmetry of the RUM whose eigenvector comprises the necessary distortions to cause each phase transition

in the structure of the parent phase, and the subscript number labels the mode. The corresponding spectroscopic symmetry is given in brackets.

It is easiest to describe the eigenvectors associated with the six RUMs in terms of translations and rotations of the SiO_4 tetrahedra with respect to a set of orthogonal axes, x, y and z. The z axis is parallel to the crystallographic c axis; the x axis is parallel to the crystallographic a axis; and the y axis is parallel to b^*. The non-degenerate modes, Γ_1^- and Γ_3^-, both comprise purely rotations of the SiO_4 tetrahedra about the z axis. The two doubly-degenerate modes, Γ_5^- and Γ_6^-, are mixtures of translations and rotations of the tetrahedra along and about both the x and y axes.

For a non-degenerate mode there can only be one possible space group arising from the distortions associated with the mode eigenvector, but for a degenerate mode, a number of space groups will be possible because the associated eigenvectors can not be uniquely defined and are free to mix together. For each of the doubly-degenerate modes at Γ in HP tridymite, there are three possible space

group symmetries that may be obtained from the HP space group, depending on how the components of the two associated eigenvectors are combined. Therefore, the RUMs at Γ in HP tridymite create the possibility for phase transitions to structures with eight different space groups, two from the two non-degenerate modes and three from each of the doubly-degenerate modes, and these are listed by Stokes and Hatch (1988). The eight possible crystal structures are illustrated in Fig. 3. In the four structures on the right of the figure, the uppermost being due to the Γ_3^- mode and the other three to the Γ_6^- mode, the distortions in both layers of the unit cell are the same and so the top layer masks the view of the bottom layer. In the other four structures, due to the Γ_1^- and Γ_5^- modes, the distortions in the two layers are opposite and so in each case the bottom layer is partially visible. This is the only difference which distinguishes between the two non-degenerate Γ_1^- and Γ_3^- modes, whose eigenvectors are both purely composed of rotations about the z axis, which distort the hexagonal rings into ditrigonal or "D-shaped" rings. It is the Γ_1^- mode which has the correct symmetry to cause a phase transition from the HP phase to a structure with the space group symmetry of the LHP phase, $P6_322$, Fig. 4.

The specific heat capacity of tridymite as a function of temperature was measured by Cellai et al. (1994) and de Dombal and Carpenter (1993) using differential scanning calorimetry (DSC). Both studies report an anomaly in the heat capacity around 700 K. Cellai et al. (1994) were able to identify this as a well-defined discontinuity in the excess specific heat at 680 K, consistent with the second-order character of the HP-LHP phase transition, but with a tail on the high-temperature side persisting up to 750 K. This indicates the presence of extra entropy in the system, which may be attributed to the softening of the RUM as the transition temperature is approached from above.
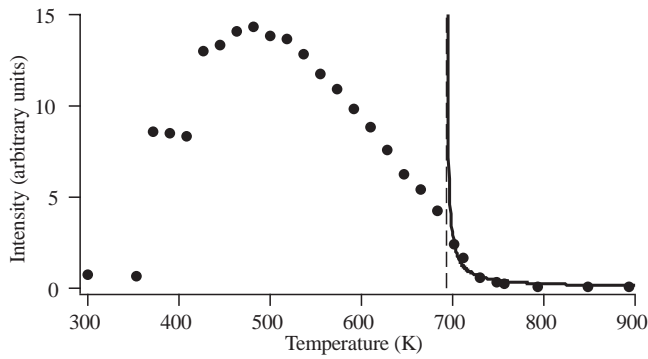
Fig. 5 The variation with temperature of the integrated intensity (arbitrary scale) of the $\bar{2}41$ reflection (hexagonal setting), which is 041 in the orthorhombic setting, for an annealed sample of tridymite from the Steinbach meteorite. The data are taken from Cellai et al. (1994). The *curve* shows a fit to the intensity of the diffuse scattering from the softening Γ_1^- RUM, at the position of this systematic absence in the HP phase

The softening of the Γ_1^- RUM is also evident from measurements of the scattering intensity recorded at the position of the $\bar{2}41$ reflection, Fig. 5, in single crystal X-ray diffraction patterns, (Cellai et al. 1994). The $\bar{2}41$ reflection is systematically absent for the HP phase, due to the presence of the c-glide in the crystal structure, but it is present for the LHP phase. The intensity of the scattering at the position of the $\bar{2}41$ reflection is negligible at temperatures well above the HP–LHP transition, but begins to rise around 750 K. The scattering is initially diffuse in character but becomes sharper below 680 K.

The frequency, ω, of a soft mode decreases as the critical temperature T_c is approached from above, i.e. for $T>T_c$:

$$\omega^2 \propto (T - T_c)$$

(see for example Dove 1993, 1997b) and the intensity, I, of diffuse scattering from a soft mode will follow as

$$I \propto \frac{k_B T}{\omega^2} \propto \frac{k_B T}{(T - T_c)}.$$

Figure 5 shows a convincing fit of this function to the experimental data for the intensity of the $\bar{2}41$ reflection, giving $T_c=693\pm2$ K, which is within the range of experimental values for the HP–LHP phase transition (particularly when experimental calibrations are taken into account). Thus we identify the intensity of the $\bar{2}41$ reflection as arising from diffuse scattering above 693 K and from Bragg scattering below.

This interpretation of the experimental observations surrounding the HP–LHP phase transition is somewhat different, at least in presentation, from that given by Cellai et al. (1994) as encapsulated in Fig. 1. Here, the emergence of intensity at the positions of systematic absences at 750 K was taken to signify the violation of the $P6_3/mmc$ space group symmetry of the HP phase, and therefore evidence that the HP–LHP phase transition had occurred. To explain the second-order phase transition characterised by

the specific heat anomaly at the lower temperature of 680 K, a separate short-range order - long-range order (sro-lro) phase transition within the LHP phase was proposed, Fig. 1. This transition was characterised by the change from a crystal structure composed of "microdomains of LHP" to the LHP phase proper. This interpetation, however, leaves the second-order HP–LHP transition without an associated heat capacity anomaly, whereas there is one associated with the subtle sro-lro transition. In fact, since the diffuse scattering described will arise from large-amplitude fluctuations involving the RUM distortion associated with the soft mode giving the LHP phase, both models point to the growth in the short-range order on cooling towards the temperature at which the long-range order sets in.

The LHP-OC transition

In contrast to the HP-LHP transition, the LHP-OC transition is easily recognised in the lattice parameter graphs as a result of the *a-b* splitting which occurs on transformation from a hexagonal to orthorhombic crystal structure. The results from four X-ray diffraction studies (Cellai et al. 1994; de Dombal and Carpenter 1993; Graetsch and Flörke 1991; Kihara 1978) place the transition temperature at approximately 620 K. In common with the previous phase transition, this displacive phase transition does not change the volume of the primitive unit cell, except for small changes in the lattice parameters, which still contains just four SiO_4 tetrahedra. Therefore, this transition is also due to a zone-centre soft mode. There are two doubly-degenerate modes at Γ for LHP tridymite, the Γ_5 and Γ_6 modes. These are closely related to the Γ_5^- and Γ_6^- modes in the HP phase. The Γ_5 mode has the correct symmetry to cause a phase transition from the LHP phase to a structure with the same space group symmetry as the OC phase, $C222$ (Fig. 4). This doubly-degenerate mode could also cause a transition to a $P2_1$ structure. In the HP phase, the Γ_5^- mode could produce a third possibility, a $Cmc2_1$ structure, see Fig. 3, but the mirror planes and c-glide of the HP structure, $P6_3/mmc$, are lost following the transition to the LHP structure, $P6_322$, and so a $Cmc2_1$ structure cannot be obtained as a subgroup of the LHP phase.

The OC-OS-OP transitions

The OS and OP phases are $n{\times}1{\times}1$ supercells of the OC structure, where n is not necessarily an integer in the incommensurately modulated OS phase, and $n=3$ for the OP phase (Kihara 1977). For the OS phase, n increases as the temperature lowers and values for n have been recorded in the range 7–12 (Dollase and Baur 1976; Nukui et al. 1978). The relationship between the OC, OS and OP phases is described in greater detail in Pryde and Heine (1998) in which the unknown structure of the OS phase is derived using the RUM approach.

The transition from the OC phase to an $n \times 1 \times 1$ superstructure with a primitive cell, such as the OP or OS phase, is due to a soft mode in the OC phase with wave vector along $(\xi,0,0)$, i.e. $\mathbf{k}=\mu\mathbf{a}^*$ where $\mu=1/n$. This line in reciprocal space is conventionally labelled Σ. A RUM analysis on the OC phase shows that there is a single RUM for all general wave vectors along Σ. There are only two possible symmetries for a Σ mode in the OC space group (Cracknell et al. 1979). A Σ_1 mode will not change the space group symmetry and so the symmetry of the soft mode must be Σ_2 (Fig. 4).

The OS phase consists of a set of structures, each derived from the OC phase, but with a different modulating wave vector. The OP phase corresponds to another such structure. The first structure in the OS phase can be derived continuously from the OC phase preceding it. However, the subsequent structures in the OS phase, and following them, the OP phase, cannot be derived continuously from the structure preceding them, since this will be a "sibling" structure, rather than the parent OC phase. This suggests that the initial OC-OS transition will be continuous, followed by a series of first order transitions between the structures of the OS phase and eventually another first order transition to the OP phase. It should be remembered that the OP phase is only observed in samples which have been annealed in the stability field of the HP phase. Those that have not proceed directly from the OS phase to the MC phase.

Both de Dombal and Carpenter (1993) and Cellai et al. (1994) report the results of DSC performed on unannealed tridymite samples from the Steinbach meteorite and therefore these results do not feature the OP phase. In the case of Cellai et al. (1994), the experiment was repeated having annealed the sample, and the OP phase was then observed. The results from the unannealed sample show a second order heat capacity anomaly accompanying the OC-OS transition at 500 K, followed by a series of four or five very small peaks in the heat capacity on cooling, characteristic of first order phase transitions, prior to the transition to MC tridymite. The largest and sharpest of these peaks occurs at approximately 440 K in both experiments. Therefore, despite this seemingly complicated sequence of incommensurate phases with different modulations, it appears to be consistent and reproducible, although this may in part be due to the common origin of the samples in the two experiments. Following the heat treatment, the OC-OS phase transition is found to occur at the slightly higher temperature of 520 K. On cooling there are then just two further heat capacity anomalies within the OS phase, including the same small but sharp peak at 440 K observed for the unannealed samples. The transition from OS to OP tridymite, at 420 K, is characterised by a relatively large first order peak in the heat capacity. This peak is approximately 30 times the height of the peak at 440 K, and is by far the largest feature in the heat capacity observed in the temperature range discussed so far. This suggests that the structure resulting from the $\mathbf{k}=1/3\mathbf{a}^*$ modulation of the OC phase represents a particularly stable structure, with respect to other possible modulations. Cellai et al. (1994) calculated the transition enthalpy associated with this peak to be 1.2 meV (per formula unit). This is an order of magnitude smaller than the transition enthalpy for the α-β transition in cristobalite, 13.0 meV (Schmahl et al. 1992). Therefore, whilst the OS-OP transition may represent a relatively large reduction in energy for the tridymite structure, it is nevertheless still very small on the scale of phase transitions in similar crystal structures.

The volume of the tridymite structure in the OC phase is greater than 99% of the HP phase volume. Following the transition to OP tridymite, the volume of the crystal structure drops to 97.5% of the HP value. The results of the X-ray diffraction studies reported in Kihara (1978), Graetsch and Flörke (1991) and Cellai et al. (1994) show that this drop is predominantly due to a substantial reduction in the b lattice parameter. The X-ray diffraction study by de Dombal and Carpenter (1993) did not extend to temperatures low enough to show this. The other three X-ray studies also reveal a small drop in the a lattice parameter, and a slight increase in the coefficient of thermal expansion for the c lattice parameter on cooling through the OS-OP phase transition.

In summary, the continuous OC-OS phase transition and the subsequent first order transitions between structures in the OS phase are characterised by extremely small volume changes and energy differences. The first order transition from OS to OP tridymite is by contrast a relatively large scale effect for tridymite, signifying some special stability associated with the distortions due to the RUM at $\mathbf{k}=1/3\mathbf{a}^*$ compared with other wave vectors along $\mathbf{k}=\mu\mathbf{a}^*$ in the OC phase. However, the volume change and transition enthalpy associated with the OS–OP transition are still small when compared with the α-β transition in cristobalite.

The OP-MC transition

So far, each tridymite phase in the sequence extending from the HP phase has been derived from a RUM distortion of the previous phase in the sequence, with the slight modification that the OP phase is derived from the phase prior to this, i.e. the OC phase rather than the OS phase. In other words, the phases follow a single transition path from the HP phase, although this path forks below OC tridymite, see Fig. 4.

The next phase in the sequence is the C-centred monoclinic structure MC tridymite, space group Cc. The layers in the crystal structures of the OP and MC phases appear very similar (Fig. 2) comprising oval and ditrigonal (D-shaped) rings in the ratio 1:2. However, the MC phase cannot be derived directly from the OP phase via a RUM distortion. This is signalled by the presence of the c-glide in the MC structure, because this symmetry element cannot be derived from any present in the OP phase. In fact, it is the HP phase which must be used as the starting point from which to apply a RUM distortion and acquire the MC structure. The RUM which can achieve this

is the H_1 mode, located at the position (1/3,1/3,1/2) in the reciprocal space of the HP phase, see Fig. 4.

Because the MC phase cannot be derived continuously from the OP phase via a RUM distortion, the OP-MC transition will be discontinuous in nature, like the OS-OP transition for example. This is confirmed by the DSC results in de Dombal and Carpenter (1993) and Cellai et al. (1994) which both show two first order anomalies in the specific heat at approximately 380 K and 370 K. These peaks are partially merged together in the results from the unannealed tridymite specimens, but they are clearly separated in the heat capacity results obtained from the annealed sample (Cellai et al. 1994). In all the results, the peak at 380 K is several times larger than the peak at 370 K.

The presence of two anomalies suggests that there is actually an intermediate phase between the OP and MC phases. This possibility is completely consistent with the model of the tridymite phase transitions presented here. It is not possible to say what this intermediate phase is from the evidence available, and since it exists for a temperature range of only 10 K, its structure would be extremely difficult to determine experimentally. However, this phase is very likely to have a structure which can be derived from the HP structure via the distortions associated with one of its many RUMs.

The transition enthalpy for the combined transition from OP tridymite via this intermediate phase to MC tridymite was calculated to be 2.8 meV by Cellai et al. (1994). In the case of the unannealed samples, which transform from OS tridymite via the intermediate to MC tridymite without passing through the OP phase, the transition enthalpy was 4.0 meV. This is equal to the sum of the enthalpies for the OS–OP transition and the OP–MC transition (via the intermediate phase) in the annealed sample.

The reduction in volume continues, and is predominantly due to a large drop in the a lattice parameter (which corresponds to the longest cell dimension in the OP phase) since the b and c lattice parameters both experience a discontinuous increase (Graetsch and Flörke 1991, Kihara 1978). In particular, the b parameter almost recovers the value it had in the OS phase, before it fell at the transition to OP making the largest contribution to the relatively large volume reduction.

The MC-MX-1 transition

Experimental results suggest that below 340 K MX-1 tridymite is the stable phase, i.e. more stable than MC tridymite, but that there is a large energy barrier for the MC–MX-1 transition, and so in practice the MC phase is observed. For example, in order to obtain the MX-1 phase it is necessary to heat the sample out of the MC stability field, i.e. above 380 K, and then quench it to below 270 K. In addition, the stress applied to a crystal during mechanical grinding is found to assist the progress of the phase transition to MX-1 tridymite.

The only measurements of the MX-1 structure as a function of temperature come from the X-ray powder diffraction reported in Graetsch and Flörke (1991). They prepared tridymite samples in the MX-1 phase from synthetic MC tridymite using quenching and grinding independently. The measurements were taken whilst heating from room temperature up to temperatures over 900 K, and then cooling back down to room temperature. The data recorded below 340 K on the cooling run are therefore unlikely to correspond to the MX-1 phase due to the difficulty in obtaining it under such moderate circumstances. This leaves only three individual measurements of the lattice parameters in the MX-1 phase, taken between 300 and 340 K on the heating run, amongst the data of Graetsch and Flörke (1991). Although limited, the data suggest that the volume of the MX-1 phase is a little larger than the volume of the MC phase, and only the a lattice parameter of the MX-1 phase is shorter than its counterpart in the MC phase. This lattice parameter in the MX-1 phase closely corresponds to the a lattice parameter in the OC phase, Fig. 2.

The structure of the MX-1 phase is described as a cell-tripling modulation imposed on an average structure. The average structure has a unit cell which is similar in shape to the OC phase unit cell, but with a doubled c parameter, and the space group of this phase is Cc. This structure is distinct from the Cc structure of the MC phase. The modulation creates a 1×3×1 supercell of this structure, and the space group symmetry of the supercell is only $C1$ Both the average and modulated structures are shown in Fig. 2.

The derivation of the MX-1 structure from the HP phase can be divided into two parts. Firstly, a RUM distortion of the HP phase creates the Cc structure and then a RUM distortion of this average phase gives the modulated structure, the observed MX-1 structure. The RUM which causes the transition from HP tridymite to the average MX-1 structure is a quadruply-degenerate mode located at (0,0,1/2) in the reciprocal space of the HP phase. This point is conventionally labelled the A-point and the RUM is the A_3 mode. The RUM doubles the unit cell in the direction of the c axis, and the a and b axes are redefined giving a C-centred conventional unit cell. The modulation which causes the cell-tripling parallel to the b axis is due to a RUM along (0,ξ,0) in this average structure. The wave vector of the RUM is (0,2/3,0), which is one-third of the way to the next reciprocal lattice point, located at (0,2,0) rather than (0,1,0) as a result of the C-centre symmetry. The predominant components of the RUM eigenvector are rotations of the SiO_4 tetrahedra about axes parallel to the a and b axes, together with some small translations of the tetrahedra parallel to the same axes. This produces the correct form of modulated tetrahedral tilting apparent in the MX-1 structure in Fig. 2. Since the MC and MX-1 phases are descended from the HP phase via different paths, the transition between them will again be discontinuous.

Summary

The sequence of phase transitions exhibited by the tridymite structure can be better understood by approaching it from the perspective of the RUM model. By deducing the RUMs responsible for each of the displacive phase transitions, and in particular the phase from which each RUM originates, it has been possible to construct a "family tree" for the tridymite phases (Fig. 4). From this, the nature of the various phase transitions, i.e. continuous or discontinuous, can be appreciated as an artefact of the relationship between the two phases involved. When one phase can be obtained from the preceding phase in the transition sequence via a RUM distortion of this phase, the transition can proceed in a continuous fashion. If a phase is not directly descended from the preceding phase in the sequence, the transition between them will be discontinuous. Small deviations away from a perfect specimen cause variations in the behaviour observed across different tridymite samples, e.g. transition temperatures and the presence of certain phases. The work presented here provides a theoretical framework which can assist in attributing experimental observations to the correct phase transition effect, where confusion may have previously arisen.

Experimental results, such as the volume changes and transition enthalpies associated with different phase transitions, as well as practical details pertaining to the measures which need to be taken in order to observe certain tridymite phases (especially OP and MX-1 tridymite), have been considered in order to gain insights into the phase transition behaviour of tridymite. In particular these results show that the energy balance between the various tridymite phases is a very delicate one. Even subtle perturbations of these energies can have a substantial effect on the transition sequence. For example, in the case of OP tridymite, stacking faults in the crystal structure reduce the temperature range over which the phase is observed, and can even prevent it from forming at all. The fine energy balance between a large number of phases is in stark contrast to the situation observed for the structurally related silicate cristobalite in which there is just one phase transition, associated with comparatively large changes in energy and volume.

References

Cellai D, Carpenter MA, Wruck B, Salje EKH (1994) Characterization of high-temperature phase transitions in single crystals of Steinbach tridymite. Am Mineral 79:606–614

Cracknell AP, Davies BL, Miller SC, Love WF (1979) Kronecker product tables:general introduction and tables of irreducible representations of space groups. IFI/Plenum Data Company, New York

Dollase WA (1967) The crystal structure at 220 C of orthorhombic high tridymite from the Steinbach meteorite. Acta Crystallogr 23:617–623

Dollase WA, Baur WH (1976) The superstructure of meteoritic low tridymite solved by computer simulation. Am Mineral 61:971–978

de Dombal RF, Carpenter MA (1993) High-temperature phase transitions in Steinbach tridymite. Eur J Mineral 5:607–622

Dove MT (1993) Introduction to lattice dynamics. Cambridge University Press, Cambridge, UK

Dove MT, Heine V, Hammonds KD (1995) Rigid unit modes in framework silicates. Mineral Mag 59:629–639

Dove MT (1997a) Silicates and soft modes. In: Thorpe MF, Mitkova MI (eds) Amorphous insulators and semiconductors, NATO ASI series 3. High Technology (Kluwer, Amsterdam), vol 23, pp 349–383

Dove MT (1997b) Theory of displacive phase transitions in minerals. MT Dove. Am Mineral 82:213–244

Dove MT, Keen DA, Hannon AC, Swainson IP (1997) Direct measurement of the Si–O bond length and orientational disorder in β-cristobalite. Phys Chem Minerals 24:311–317

Giddy AP, Dove MT, Pawley GS, Heine V (1993) The determination of rigid unit modes as potential soft modes for displacive phase transitions in framework crystal structures. Acta Crystallogr A49:697–703

Graetsch H, Flörke OW (1991) X-ray powder diffraction patterns and phase relationship of tridymite modifications. Z Kristallogr 195:31–48

Graetsch H, Topalovic-Dierdorf I (1996) ^{29}Si MAS NMR spectrum and superstructure of modulated tridymite L3-T_O(MX-1). Eur J Mineral 8:103–113

Hammonds KD, Dove MT, Giddy AP, Heine V (1994) CRUSH:A FORTRAN program for the analysis of the rigid unit mode spectrum of a framework structure. Am Mineral 79 :1207–1209

Hammonds KD, Dove MT, Giddy AP, Heine V, Winkler B (1996) Rigid unit phonon modes and structural phase transitions in framework silicates. Am Mineral 81:1057–1079, 1996

Hoffmann W (1967) Gitterkonstanten und Raumgruppe von Tridymite bei 20 C. Naturwissenschaften 54:114

Kato K, Nukui A (1976) Die Kristallstruktur des monoklinen Tief-Tridymits. Acta Crystallogr B32:2486–2491

Kihara K (1977) An orthorhombic superstructure of tridymite existing between about 105 and 180 C. Z Kristallogr 146:185–203

Kihara K (1978) Thermal change in unit-cell dimensions, and a hexagonal structure of tridymite. Z Kristallogr 148:237–253

Löns J, Hoffmann W (1987) Zur Kristallstruktur der inkommensurablen Raumtemperaturphase des Tridymits. Z Kristallogr 178: 141–143

Nukui A, Nakazawa H, Akao M (1978) Thermal changes in monoclinic tridymite. Am Mineral 63:1252–1259

Pryde AKA, Heine V (1998) Analysis of the incommensurately modulated OS phase of SiO$_2$ tridymite. Phys Chem Minerals 25:603–610

Schmahl WW, Swainson IP, Dove MT, Graeme-Barber A (1992) Landau free energy and order parameter behaviour of the α–β phase transition in cristobalite. Z Kristallogr 201:125–145

Stokes HT, Hatch DM (1988) Isotropy subgroups of the 230 crystallographic space groups. World Scientific, Singapore

Swainson IP, Dove MT (1993) Low-frequency floppy modes in β-cristobalite. Phys Rev Lett 71:193–196

Swainson IP, Dove MT (1995) Molecular dynamics simulation of α- and β-cristobalite. J Phys Condens Matter 7:1771–1788